Approximations on $SO(3)$ by Wigner D-matrix and applications

Jie Shen[1], Jie Xu[1] and Pingwen Zhang[2]

[1]Department of Mathematics, Purdue University, West Lafayette 47907, USA
[2]LMAM & School of Mathematical Sciences, Peking University, Beijing 100871, China
Email: shen7@purdue.edu, xu924@purdue.edu, pzhang@pku.edu.cn

Abstract

We consider approximations on $SO(3)$ by Wigner D-matrix. We establish basic approximation properties of Wigner D-matrix, develop efficient numerical schemes using Wigner D-matrix for elliptic and parabolic equations on $SO(3)$, and establish corresponding optimal error estimates. Numerical examples are presented to validate the theoretical estimates and illustrate a physical application.

keywords. Wigner D-matrix, $SO(3)$, error estimate, spectral-Galerkin, polymers

AMS subject classifications. 41A30, 65N35, 65M70

1 Introduction

In most problems relevant to three-dimensional rotations, we need to express functions in the rotational group $SO(3)$. Because Wigner D-matrix is an irreducible representation of $SO(3)$, it is naturally used to expand functions in $SO(3)$, similar to Fourier expansion for periodic functions or spherical harmonic expansion for functions in spherical domains. Although originally introduced in group representation and quantum mechanics [22, 20, 24], Wigner D-matrix has now been applied to various areas [3], including image searching and analysis [6], cosmology [21], molecular biology [11], polymeric and liquid crystalline materials [23, 18, 19, 17]. The development of fast transformation between the physical and the frequency space [10] has brought great convenience to its applications.

When solving PDEs on $SO(3)$, Wigner D-matrix is often used as basis functions in a spectral-Galerkin approach. However, error estimates for such approach involving Wigner D-matrix is not yet available. The main purposes of this paper are (i) to derive a basic approximation theory for Wigner D-matrix; (ii) to derive an efficient spectral-Galerkin algorithm using Wigner D-matrix and the corresponding error estimates for solving elliptic and parabolic type equations on $SO(3)$; and (iii) to illustrate how to use spectral-Galerkin algorithm with Wigner D-matrix to simulate a worm-like chain on the spherical surface.

It is known that the accuracy of the spectral-Galerkin solution is controlled by the approximation properties of the basis functions. Analysis of this kind has been done for Fourier series and orthogonal polynomials [12, 2, 8, 9, 16]. The key property in the proof of approximation results is a derivative relation similar to that satisfied by the Jacobi polynomials.

Such a derivative relation played a key role in the error estimate of Jacobi polynomials [9, 16]. With the approximation results in hand, we then consider using Wigner D-matrix to solve elliptical and parabolic equations on $SO(3)$.

As an application, we focus on a model of polymers, where the chain propagator equation needs to be solved. The chain propagator equation is crucial for the computation of the single chain partition function [5]. The form of chain propagator equation is identical to Schrödinger equation except without the unit $i\hbar$. The space of variables depends on the symmetry of the monomers/building blocks. If they do not have spherical or axial symmetry, the differential equations are necessarily on $SO(3)$. The space of variables also depends on the geometry of the region in which the molecule is confined. An example is worm-like molecules on spherical surface [14], where the chain propagator equation is also on $SO(3)$. Other applications we plan to consider in a future work is the Smoluchowski equation which describes the evolution of density function for liquid crystals [4].

The rest of paper is organized as follows. In Sec. 2, we introduce the notations in $SO(3)$, the definition and some important relations of Wigner D-matrix. Sec. 3 is dedicated to the error estimate for approximation by Wigner D-matrix. Applications to elliptic and parabolic equations are presented in Sec. 4 where we propose efficient algorithms and derive optimal error estimates. Numerical examples are presented in Sec. 5 to validate the theoretical results and illustrate physical applications. A brief concluding remark is given in Sec. 6.

2 Wigner D-matrix

2.1 The elements of $SO(3)$

We choose a reference orthonormal frame $(\boldsymbol{e}_1, \boldsymbol{e}_2, \boldsymbol{e}_3)$ in $\mathbb{R}^3$. Each orthonormal frame $(\boldsymbol{m}_1, \boldsymbol{m}_2, \boldsymbol{m}_3)$ can be expressed by rotating $(\boldsymbol{e}_1, \boldsymbol{e}_2, \boldsymbol{e}_3)$ with $P \in SO(3)$, namely $PP^T = 1$, $|P| = 1$ and

$$(\boldsymbol{m}_1, \boldsymbol{m}_2, \boldsymbol{m}_3) = (\boldsymbol{e}_1, \boldsymbol{e}_2, \boldsymbol{e}_3)\, P.$$

The elements of P,

$$P = \begin{pmatrix} m_{11} & m_{21} & m_{31} \\ m_{12} & m_{22} & m_{32} \\ m_{13} & m_{23} & m_{33} \end{pmatrix}$$

are given by

$$m_{jk} = \boldsymbol{m}_j \cdot \boldsymbol{e}_k.$$

In the above description, P is determined by $\boldsymbol{m}_j$. We may also view $\boldsymbol{m}_j$ as functions of P.

The elements in $SO(3)$ can be expressed by Euler angles α, β, γ:

$$\begin{aligned} &P(\alpha, \beta, \gamma) \\ =& \begin{pmatrix} \cos\beta & -\sin\beta\cos\gamma & \sin\beta\sin\gamma \\ \sin\beta\cos\alpha & \cos\beta\cos\alpha\cos\gamma - \sin\alpha\sin\gamma & -\cos\beta\cos\alpha\sin\gamma - \sin\alpha\cos\gamma \\ \sin\beta\sin\alpha & \cos\beta\sin\alpha\cos\gamma + \cos\alpha\sin\gamma & -\cos\beta\sin\alpha\sin\gamma + \cos\alpha\cos\gamma \end{pmatrix}, \end{aligned} \tag{2.1}$$

where

$$\beta \in [0, \pi], \;\; \alpha, \gamma \in [0, 2\pi).$$

The uniform unit measure in $SO(3)$ is given by

$$\mathrm{d}\nu = \frac{1}{8\pi^2}\sin\beta\,\mathrm{d}\alpha\,\mathrm{d}\beta\,\mathrm{d}\gamma.$$

2.2 Differential operators

In the tangential space at P, denoted by $TSO(3)(P)$, we choose an orthonormal basis (X_1, X_2, X_3). For any differentiable function f, the directional derivatives can be calculated by

$$\frac{\mathrm{d}}{\mathrm{d}t}f(P(t)) = \sum_{i=1}^{3}\partial_{X_i}f\cdot(X_i, \frac{\mathrm{d}P}{\mathrm{d}t}).$$

Note that $PP^T = P^TP = I$. Thus we have

$$\frac{\mathrm{d}P}{\mathrm{d}t}P^T + P\frac{\mathrm{d}P^T}{\mathrm{d}t} = \frac{\mathrm{d}P^T}{\mathrm{d}t}P + P^T\frac{\mathrm{d}P}{\mathrm{d}t} = 0.$$

So we can find skew-symmetric matrices A_l, A_r such that $\mathrm{d}P/\mathrm{d}t = A_lP = PA_r$. Hence (S_1P, S_2P, S_3P) and (PS_1, PS_2, PS_3) are two orthonormal basis of $TSO(3)(P)$, where

$$S_1 = \begin{pmatrix} 0 & 0 & 0 \\ 0 & 0 & -1 \\ 0 & 1 & 0 \end{pmatrix}, S_2 = \begin{pmatrix} 0 & 0 & 1 \\ 0 & 0 & 0 \\ -1 & 0 & 0 \end{pmatrix}, S_3 = \begin{pmatrix} 0 & -1 & 0 \\ 1 & 0 & 0 \\ 0 & 0 & 0 \end{pmatrix}. \tag{2.2}$$

When we choose $X_k = S_kP$, we denote $J_k = \partial_{X_k}$; when we choose $X'_k = PS_k$, we denote $L_k = \partial_{X'_k}$. Intuitively, J_k represents the derivative of the infinitesimal rotation about $\boldsymbol{e}_k$, and L_k represents the derivative of the infinitesimal rotation about $\boldsymbol{m}_k$. We can also write

$$J_kf(P) = \lim_{t\to 0}\frac{f(\exp(tS_k)P) - f(P)}{t}, \quad L_kf(P) = \lim_{t\to 0}\frac{f(P\exp(tS_k)) - f(P)}{t}. \tag{2.3}$$

By computing the derivatives of P about Euler angles, we can write J_k and L_k by Euler angles:

$$J_1 = \frac{\partial}{\partial\alpha}, \tag{2.4}$$

$$J_2 = \frac{\cos\alpha}{\sin\beta}\left(\frac{\partial}{\partial\gamma} - \cos\beta\frac{\partial}{\partial\alpha}\right) - \sin\alpha\frac{\partial}{\partial\beta}, \tag{2.5}$$

$$J_3 = \frac{\sin\alpha}{\sin\beta}\left(\frac{\partial}{\partial\gamma} - \cos\beta\frac{\partial}{\partial\alpha}\right) + \cos\alpha\frac{\partial}{\partial\beta}, \tag{2.6}$$

$$L_1 = \frac{\partial}{\partial\gamma}, \tag{2.7}$$

$$L_2 = \frac{-\cos\gamma}{\sin\beta}\left(\frac{\partial}{\partial\alpha} - \cos\beta\frac{\partial}{\partial\gamma}\right) + \sin\gamma\frac{\partial}{\partial\beta}, \tag{2.8}$$

$$L_3 = \frac{\sin\gamma}{\sin\beta}\left(\frac{\partial}{\partial\alpha} - \cos\beta\frac{\partial}{\partial\gamma}\right) + \cos\gamma\frac{\partial}{\partial\beta}. \tag{2.9}$$

Using (2.4)-(2.9), we can verify the following properties. First, we have

$$J_1^2 + J_2^2 + J_3^2 = L_1^2 + L_2^2 + L_3^2 \triangleq L^2 = J^2. \tag{2.10}$$

Second, the operators satisfy

$$[J_{k_1}, J_{k_2}] = J_{k_1}J_{k_2} - J_{k_2}J_{k_1} = -\epsilon_{k_1k_2k_3}J_{k_3}, \quad [L_{k_1}, L_{k_2}] = \epsilon_{k_1k_2k_3}L_{k_3}, \tag{2.11}$$

where

$$\epsilon_{k_1k_2k_3} = \begin{cases} 1, & (k_1k_2k_3) = (123), (231), (312), \\ -1, & (k_1k_2k_3) = (132), (213), (321), \\ 0, & \text{otherwise.} \end{cases}$$

Thus we can verify that

$$[L^2, J_k] = [L^2, L_k] = [J_{k_1}, L_{k_2}] = 0.$$

The derivatives of m_{ij} are given by

$$J_{k_1}m_{lk_2} = \epsilon_{k_1k_2k_3}m_{lk_3}, \quad L_{k_1}m_{k_2l} = \epsilon_{k_1k_2k_3}m_{k_3l}. \tag{2.12}$$

The operators satisfy the equation of integration by parts in $SO(3)$,

$$\int \mathrm{d}\nu f(J_kg) = -\int \mathrm{d}\nu (J_kf)g, \quad \int \mathrm{d}\nu f(L_kg) = -\int \mathrm{d}\nu (L_kf)g. \tag{2.13}$$

2.3 Wigner D-matrix

By (2.13), the operators iJ_k and iL_k are symmetric on $L^2(SO(3))$, where $i = \sqrt{-1}$ is the imaginary unit. Also $-L^2, iJ_1, iL_1$ are mutually commutative, so we may consider their common eigenfunctions,

$$-L^2\phi = \lambda\phi, iJ_1\phi = m\phi, iL_1\phi = m'\phi. \tag{2.14}$$

By solving the eigenfunction problem, we obtain that $\lambda = j(j+1),\ j \geq |m|, |m'|,\ j, m, m' \in \mathbb{Z}$, and the corresponding eigenfunction gives the Wigner D-matrix,

$$D^j_{mm'} = \exp(-im\alpha)d^j_{mm'}(\beta)\exp(-im'\gamma), \tag{2.15}$$

where

$$d^j_{mm'}(\beta) = (-1)^\nu \binom{2j-k}{k+a}^{1/2} \binom{k+b}{b}^{-1/2} \left(\sin\frac{\beta}{2}\right)^a \left(\cos\frac{\beta}{2}\right)^b P_k^{(a,b)}(\cos\beta).$$

In the above, $k = j - \max(|m|, |m'|)$, $a = |m - m'|$, $b = |m + m'|$,

$$\nu = \begin{cases} 0, & \text{if } m' \leq m, \\ m' - m, & \text{if } m' > m, \end{cases}$$

and

$$P_k^{(a,b)}(x) = \sum_s \binom{k+a}{s}\binom{k+b}{k-s}\left(\frac{x-1}{2}\right)^{n-s}\left(\frac{x+1}{2}\right)^s$$

is the Jacobi polynomial. When $m' = 0$, the Wigner-D matrix becomes the spherical harmonic functions, i.e.,

$$D^j_{m0} = Y^j_m,$$

where Y^j_m are the spherical harmonic functions. By the theory of group representation [20], we have

Proposition 2.1. *$D^j_{mm'}$ is a complete orthogonal basis of $L^2(SO(3))$.*

In fact, the orthogonality can also be verified directly by that of Jacobi polynomials. If $m_1 \neq m_2$ or $m'_1 \neq m'_2$, it is obvious that $D^{j_1}_{m_1 m'_1}$ and $D^{j_2}_{m_2 m'_2}$ are orthogonal. And we have

$$\int \mathrm{d}\nu\, D^{j_1}_{mm'} D^{j_2 *}_{mm'} = C \int_{-1}^{1} \mathrm{d}x\, (1-x)^a (1+x)^b P^{(a,b)}_{k_1}(x) P^{(a,b)}_{k_2}(x) = C\delta_{j_1 j_2}.$$

The Wigner D-matrix also satisfies the following differential relations: define $L_\pm = iL_2 \mp L_3$, $J_\pm = iJ_2 \pm J_3$, then

$$L_\pm D^j_{mm'} = \sqrt{j(j+1) - m'(m' \pm 1)} D^j_{m,m'\pm 1}, \tag{2.16}$$

$$J_\pm D^j_{mm'} = \sqrt{j(j+1) - m(m \pm 1)} D^j_{m\pm 1,m'}. \tag{2.17}$$

The relations (2.14), (2.16) and (2.17) are crucial in the error estimate.

3 Approximation error by Wigner-D matrix

We shall only consider the operator L_k, since J_k can be studied in exactly the same manner.

We define the H^p space on $SO(3)$ by

$$H^p(SO(3)) = \{f(P) : L_{j_1} \dots L_{j_p} f \in L^2(SO(3))\}, \tag{3.1}$$

with the semi-norm and norm

$$|f|_p^2 = \sum_{j_r = 1,2,3} |L_{j_1} \dots L_{j_p} f|^2, \quad ||f||_p^2 = \sum_{k \le p} |f|_p^2. \tag{3.2}$$

Denote $||f|| = ||f||_0$.

Since $\{D^j_{mm'}\}$ is a complete orthogonal basis, for $f(P) \in L^2(SO(3))$, we may write

$$f(P) = \sum_{0 \le |m|,|m'| \le j} \hat{f}^j_{mm'} D^j_{mm'}.$$

If $f \in H^1$, by (2.14) and (2.16), we have

$$\sum_{r=1}^{3} ||L_r f||^2 = \sum_{0 \le |m|,|m'| \le j} j(j+1) |\hat{f}^j_{mm'}|^2.$$

Recall that L^2 is defined in (2.10). Thus, for $f \in H^{2k}$,

$$||(L^2)^k f||^2 = \sum_{0 \le |m|,|m'| \le j} (j(j+1))^{2k} |\hat{f}^j_{mm'}|^2, \tag{3.3}$$

and for $f \in H^{2k+1}$,

$$\sum_{r=1}^{3} ||L_r (L^2)^k f||^2 = \sum_{0 \le |m|,|m'| \le j} (j(j+1))^{2k+1} |\hat{f}^j_{mm'}|^2. \tag{3.4}$$

Next we estimate the derivatives $L_{j_1}\dots L_{j_p}f$. We can write

$$L_+^2 f = \sum_{0\le|m+1|,|m'|\le j} \sqrt{[j(j+1)-m(m+1)][j(j+1)-(m+1)(m+2)]}\hat{f}^j_{mm'}D^j_{m+2,m'}.$$

Therefore,

$$||L_+^2 f||^2 \le \sum_{0\le|m+1|,|m'|\le j} (j(j+1))^2|\hat{f}^j_{mm'}|^2 \le ||L^2 f||^2.$$

Similarly, we can derive $||L_{s_1}L_{s_2}f|| \le ||L^2 f||$ for $s_1, s_2 \in \{1,+,-\}$. Thus, for $j_r \in \{1,2,3\}$, we have

$$||L_{j_1}\dots L_{j_p}f||^2 \le C(p) \sum_{0\le|m|,|m'|\le j} (j(j+1))^p|\hat{f}^j_{mm'}|^2, \tag{3.5}$$

where $C(p) = 2^p$.

Denote

$$X_N = \text{span}\{D^j_{mm'} : j \le N\}. \tag{3.6}$$

Define the projection operator π_N as

$$(\pi_N f - f, g) = 0, \quad \forall g \in X_N. \tag{3.7}$$

Then π_N can be written as

$$\pi_N f = \sum_{0\le|m|,|m'|\le j\le N} \hat{f}^j_{mm'}D^j_{mm'}. \tag{3.8}$$

Now we can reach an error estimate of the π_N.

Theorem 3.1. *For any $f \in H^p(SO(3))$ and $k \le p \le N$,*

$$||L_{j_1}\dots L_{j_k}(\pi_N f - f)|| \le CN^{k-p}|f|_p. \tag{3.9}$$

Proof. Using (3.5), (3.3), and (3.4), we have

$$\begin{aligned}||L_{j_1}\dots L_{j_k}(\pi_N f - f)||^2 \le& C \sum_{j>N,0\le|m|,|m'|\le j} (j(j+1))^{2k}|\hat{f}^j_{mm'}|^2 \\ \le& \frac{C}{(N(N+1))^{2p-2k}} \sum_{j>N,0\le|m|,|m'|\le j} (j(j+1))^{2p}|\hat{f}^j_{mm'}|^2 \\ \le& CN^{2k-2p}|f|_p^2.\end{aligned}$$

□

4 Applications

We shall consider two problems in this section: one is an elliptic equation and the other is a parabolic equation.

4.1 Elliptic equation

Consider

$$-L_i A_{ij} L_j u + b_i L_i u + cu = f, \tag{4.1}$$

with $A_{ij}(P), b_i(P), c(P) \in L^\infty(SO(3))$, $f(P) = L^2(SO(3))$, and the conventional notation about repeated indices is used. We also assume that the matrix

$$\begin{pmatrix} A_{ij} & b_i \\ b_j & c \end{pmatrix}$$

is symmetric positive definite at each $P \in SO(3)$, with the minimal eigenvalue $\geq \lambda > 0$. Under this assumption, the bilinear form

$$a(u, v) = \int (A_{ij} L_i v L_j u + b_i v L_i u + cuv) \mathrm{d}\nu \tag{4.2}$$

is continuous and coercive about the H^1 norm in $SO(3)$, namely,

$$\begin{aligned} & a(u, v) \leq C\|u\|_1 \|v\|_1, \quad \forall u, v \in H^1; \\ & \lambda \|u\|_1 \leq a(u, u), \quad \forall u \in H^1. \end{aligned} \tag{4.3}$$

The weak form of the equation is to find $u \in H^1(SO(3))$ such that

$$a(u, v) = (f, v), \quad \forall v \in H^1(SO(3)). \tag{4.4}$$

By the Lax-Milgram lemma, there exists a unique solution for the above problem.

4.1.1 Regularity

We first establish a regularity result for (4.4).

The following two lemmas are similar to the elliptical equations in $\mathbb{R}^n$. The difference quotient has the following estimate.

Lemma 4.1. *Let $L_k^h f(P) = [f(P \exp(hS_k)) - f(P)]/h$, where S_k are given in (2.2).*

A. Assume $1 \leq p \leq \infty$ and $f \in W^{1,p}$. Then

$$||L_k^h f||_{L^p} \leq C||L_k f||_{L^p}. \tag{4.5}$$

B. Assume $1 < p \leq \infty$, $f \in L^p$, and there exists a constant C such that $||L_k^h f||_{L^P} \leq C$ for all h and $k = 1, 2, 3$. Then $f \in W^{1,p}$, and

$$||L_k f||_{L^p} \leq C, \quad k = 1, 2, 3. \tag{4.6}$$

Proof. A. If $f \in W^{1,p}$, then for every $P \in SO(3)$,

$$f(P \exp(hS_k)) - f(P) = h \int_0^1 \mathrm{d}t L_k f(P \exp(thS_k)).$$

Therefore

$$\begin{aligned} \int \mathrm{d}\nu |L_k^h f|^p &\leq C \int \mathrm{d}\nu \int_0^1 \mathrm{d}t |L_k f(P \exp(thS_k))|^p \\ &\leq C||L_k f||_{L^P}. \end{aligned}$$

B. Let $\phi \in C^\infty$. We have

$$\int \mathrm{d}\nu f L_k^h \phi = -\int \mathrm{d}\nu L_k^h f \phi.$$

Note that L_k^h is bounded in L^p. Thus we can choose a subsequence such that $L_k^{h_l} f \rightharpoonup g$ weakly in L^p. Then

$$\int \mathrm{d}\nu f L_k \phi = \lim_{l\to\infty} \int \mathrm{d}\nu f L_k^{h_l} \phi = -\lim_{l\to\infty} \int \mathrm{d}\nu L_k^{h_l} f \phi = -\int \mathrm{d}\nu g \phi,$$

indicating that $g = L_k f$ in L^p. Hence we deduce that $f \in W^{1,p}$.

□

Lemma 4.2. *Assume $A_{ij}, b_i \in W^{1,\infty}$ and $c \in L^\infty$. Let u be the solution of (4.4) with $f = g \in L^2$, then $u \in H^2$ and*

$$||u||_2 \leq C||g||_0. \tag{4.7}$$

Here the constant C depends on $||A_{ij}||_{W^{1,\infty}}, ||b_i||_{W^{1,\infty}}, ||c||_{L^\infty}$.

Proof. Substituting v with $L_k^{-h} v$ in (4.4), we obtain

$$\int \mathrm{d}\nu A_{ij} L_i u L_j L_k^{-h} v = \int \mathrm{d}\nu (g - (c - L_i b_i) u + b_i L_i u) L_k^{-h} v. \tag{4.8}$$

From (2.3), we can deduce that

$$(L_j L_k^h - L_k^h L_j) v = \epsilon_{jkl} \frac{\sin h}{h} L_l v(P \exp(hS_2)) - \frac{1-\cos h}{h} L_j v(P\exp(hS_2)).$$

Take $(j,k) = (1,2)$ for example. Denote $R(t,h) = \exp(-hS_2)\exp(tS_1)\exp(hS_2)$. Then we have

$$\begin{aligned}
\lim_{t\to 0} \frac{1}{t}(R(t,h) - I) &= \lim_{t\to 0} \frac{1}{t} \begin{pmatrix} \cos^2 h + \sin^2 h \cos t - 1 & -\sin h \sin t & \cos h \sin h (1-\cos t) \\ \sin h \sin t & \cos t - 1 & -\cos h \sin t \\ \cos h \sin h (1 - \cos t) & \cos h \sin t & \cos^2 h \cos t + \sin^2 h - 1 \end{pmatrix} \\
&= \begin{pmatrix} 0 & -\sin h & 0 \\ \sin h & 0 & -\cos h \\ 0 & \cos h & 0 \end{pmatrix} \\
&= S_3 \sin h + S_1 \cos h.
\end{aligned}$$

Hence,

$$\begin{aligned}
h(L_1 L_2^h - L_2^h L_1) v =& \lim_{t\to 0} \frac{1}{t}[v(P\exp(tS_1)\exp(hS_2)) - v(P\exp(hS_2)\exp(tS_1))] \\
=& \lim_{t\to 0} \frac{1}{t}[v(P\exp(hS_2)R(t,h)) - v(P\exp(hS_2))] \\
&- \lim_{t\to 0} \frac{1}{t}[v(P\exp(hS_2)\exp(tS_1)) - v(P\exp(hS_2))] \\
=& \sin h L_3 v(P\exp(hS_2)) - (1-\cos h) L_1 v(P\exp(hS_2)).
\end{aligned}$$

The left side of (4.8) can be rewritten as

$$\begin{aligned}
&\int \mathrm{d}\nu A_{ij} L_i u L_j L_k^{-h} v \\
&\quad = \int \mathrm{d}\nu A_{ij} L_i u \Big[L_k^{-h} L_j v + \epsilon_{jkl} \frac{\sin h}{h} L_l v(P\exp(-hS_k)) + \frac{1-\cos h}{h} L_j v(P\exp(-hS_k)) \Big] \\
&\quad = \int \mathrm{d}\nu \; - L_k^h (A_{ij} L_i u) L_j v \\
&\qquad + A_{ij} L_i u \Big[\epsilon_{jkl} \frac{\sin h}{h} L_l v(P\exp(-hS_k)) + \frac{1-\cos h}{h} L_j v(P\exp(-hS_k)) \Big] \\
&\quad = \int \mathrm{d}\nu \; - A_{ij}(P\exp(hS_1)) L_k^h L_i u L_j v - L_k^h A_{ij} L_i u L_j v \\
&\qquad + A_{ij} L_i u \Big[\epsilon_{jkl} \frac{\sin h}{h} L_l v(P\exp(-hS_k)) + \frac{1-\cos h}{h} L_j v(P\exp(-hS_k)) \Big].
\end{aligned}$$

Thus

$$\begin{aligned}
&\int \mathrm{d}\nu A_{ij}(P\exp(hS_1)) L_k^h L_i u L_j v \\
&\quad = \int \mathrm{d}\nu \; - L_k^h A_{ij} L_i u L_j v - (g - (c + L_i b_i) u - b_i L_i u) L_k^{-h} v \\
&\qquad + A_{ij} L_i u \Big[\epsilon_{jkl} \frac{\sin h}{h} L_l v(P\exp(-hS_k)) + \frac{1-\cos h}{h} L_j v(P\exp(-hS_k)) \Big] \\
&\quad \le C_1(||u||_1 + ||g||_0)||Lv||_0.
\end{aligned}$$

Then we substitute v with $L_k^h u$ in the above, which yields

$$\begin{aligned}
\lambda ||L_k^h L u||_0^2 \le & \int \mathrm{d}\nu A_{ij}(P\exp(hS_1)) L_k^h L_i u L_k^h L_j u \\
= & \int \mathrm{d}\nu A_{ij}(P\exp(hS_1)) L_k^h L_i u \Big[L_j L_k^h u \\
& - \epsilon_{jkl} \frac{\sin h}{h} L_l u(P\exp(hS_k)) + \frac{1-\cos h}{h} L_j u(P\exp(hS_k)) \Big] \\
\le & C_1(||u||_1 + ||g||_0)||L L_k^h u||_0 + C_2 ||u||_1 ||L_k^h L u||_0 \\
\le & C_1(||u||_1 + ||g||_0)(||L_k^h L u||_0 + C_3||u||_1) + C_2||u||_1||L_k^h L u||_0 \\
\le & C_4(||u||_1 + ||g||_0)(||L_k^h L u||_0 + 1).
\end{aligned}$$

Hence $||L_k^h L u||_0 \le C_5(||u||_1 + ||g||_0)$ with $C_5 = C_4/2\lambda + \sqrt{(C_4/2\lambda)^2 + C_4/\lambda}$, which implies $u \in H^2$ and

$$||u||_2 \le C_5(||u||_1 + ||g||_0).$$

Finally, we have $\lambda ||u||_1^2 \le a(u,u) = (u,g) \le ||u||_0 ||g||_0$. Therefore $||u||_1 \le (1/\lambda)||g||_0$ and (4.7) holds. □

Corollary 4.3. *Assume $A_{ij}, b_i \in W^{k+1,\infty}$ and $c \in W^{k,\infty}$. If u is the solution of (4.4) with $f = g \in H^k$, then $u \in H^{k+2}$ and*

$$||u||_{k+2} \le C||g||_k. \tag{4.9}$$

Proof. We prove by induction. Suppose (4.9) holds for $0, \dots, k-1$. Then $u \in H^{k+1}$ and $||u||_{k+1} \le C||g||_{k-1}$. Since the coefficients and the right-hand term have better smoothness, we can take derivatives on both sides of the equation,

$$L_{p_1} \dots L_{p_k}(L_i A_{ij} L_j u + b_i L_i u + cu) = L_{p_1} \dots L_{p_k} g.$$

Denote $u' = L_{p_1} \dots L_{p_k} u$. By using (2.11), we can rewrite the above equation as

$$L_i A_{ij} L_j u' + b_i L_i u' + cu' = g'.$$

where $g' \in L^2$ and

$$||g'|| \le C(||u||_{k+1} + ||g||_k) \le C(||g||_{k-1} + ||g||_k) \le C||g||_k.$$

By Lemma 4.2, $u' \in H^2$ and $||u'||_2 \le C||g'|| \le C||g||_k$. Since p_k are arbitrary, we have $||u||_{k+2} \le C||g||_k$. □

4.1.2 Error estimate

The spectral-Galerkin method for (4.4) is: Find $u_N \in X_N$ such that

$$a(u_N, v_N) = (f, v_N), \quad \forall v_N \in X_N. \tag{4.10}$$

Again the wellposedness of the above problem is assured by the Lax-Milgram lemma. As for the error estimate, we have

Theorem 4.4. *Assume $A_{ij}, b_i \in W^{k+1,\infty}$, $c \in W^{k,\infty}$ and $f \in H^k$, where k is a nonnegative integer. If u is the solution of (4.4) and u_N is that of (4.10), then*

$$||u - u_N||_\nu \le CN^{\nu-k-2}||f||_k, \quad \forall \nu \in [0,1]. \tag{4.11}$$

Proof. We first show the result with $\nu = 1$. We derive from (4.4) and (4.10) that

$$a(u - u_N, v_N) = 0, \quad \forall v_N \in X_N.$$

By (4.3) and Cea's lemma, we immediately derive

$$||u - u_N||_1 \le C \inf_{v_N \in X_N} ||u - v_N||_1.$$

Define the projection operator π_N^1 as

$$(\pi_N^1 u - u, v_N) + (L_j(\pi_N^1 u - u), L_j v_N) = 0, \quad \forall v_N \in X_N. \tag{4.12}$$

It can be verified by (3.8), (2.14) and (2.16) that the above equality holds when substituting $\pi_N^1 u$ with $\pi_N u$, thus $\pi_N^1 = \pi_N$. Therefore, if $u \in H^m(SO(3))$, we have

$$\inf_{v_N \in X_N} ||u - v_N||_1 \le ||u - \pi_N u||_1 \le CN^{1-m}|u|_m. \tag{4.13}$$

Hence, we obtain the result for $\nu = 1$ by combining the above and the regularity result in Corollary 4.3.

Next, we prove the result for $\nu = 0$ using a standard duality argument. We write

$$||u - u_N||_0 = \frac{\sup(u - u_N, g)}{||g||_0}.$$

Denote by φ_g the solution of $a(v, \varphi_g) = (v, g)$, $\forall v$. Let $v = u - u_N$. Combined with $a(u - u_N, \pi_N \varphi_g) = 0$, (3.9), and (4.7), we obtain

$$\begin{aligned}(u - u_N, g) =& a(u - u_N, \varphi_g - \pi_N \varphi_g)\\ \le& C||u - u_N||_1 ||\varphi_g - \pi_N \varphi_g||_1\\ \le& CN^{-1}||u - u_N||_1 ||\varphi_g||_2\\ \le& CN^{-1}||u - u_N||_1 ||g||_0.\end{aligned}$$

Thus by (4.13) and (4.9),

$$||u - u_N||_0 \le CN^{-1}||u - u_N||_1 \le CN^{-k-2}|u|_{k+2} \le CN^{-k-2}||f||_k. \tag{4.14}$$

Finally, the result for $\nu \in (0, 1)$ can be obtained by a standard space interpolation [1]. □

4.1.3 Implementation

Here we discuss how to solve (4.10) numerically. Write

$$u_N = \sum_{|m|,|m'|\le j\le N} \hat{u}^j_{mm'} D^j_{mm'}.$$

1. If the coefficients A_{kl}, b_k, c are constant, it follows from (2.14) and (2.16) that

$$(A_{kl} L_k u_N, L_l D^j_{mm'}) + (b_k L_k u_N, D^j_{mm'}) + (c u_N, D^j_{mm'}) \tag{4.15}$$

is depends linearly on $\hat{u}^j_{mm'}$, $\hat{u}^j_{m,m'\pm1}$, $\hat{u}^j_{m,m'\pm2}$. Thus we group $\hat{u}^j_{mm'}$ according to the indices j and m. For fixed (j, m), we can solve $\hat{u}^j_{mm'}$ from a pentadiagonal linear equations with $2j + 1$ variables,

$$(M^j_m)_{m'p'} \hat{u}^j_{mp'} = \hat{f}^j_{mm'}, \quad -j \le |m'|, |p'| \le j,$$

which can be done by LU factorization. Denote

$$C_\pm(j, m') = \sqrt{j(j+1) - m'(m' \pm 1)}.$$

Then the nonzero elements in the matrix M^j_m can be computed by (2.14) and (2.16), given as follows (where $i = \sqrt{-1}$),

$$\begin{aligned}(M^j_m)_{m'm'} =& A_{11} m'^2 + \frac{1}{2}(A_{22} + A_{33})(j(j+1) - m'^2) + i b_1 m' + c,\\ (M^j_m)_{m',m'\pm1} =& \frac{1}{2} C_\pm(j, m')[(2m' \pm 1)(-A_{12} \pm i A_{13}) + (i b_2 \pm b_3)],\\ (M^j_m)_{m',m'\pm2} =& \frac{1}{4}(A_{22} - A_{33} \mp 2i A_{23}) C_\pm(j, m') C_\pm(j, m' \pm 1).\end{aligned}$$

2. Generally, A_{kl}, b_k, c are not constant. In this case, we first notice that (4.15) can be computed efficiently from $\hat{u}^j_{mm'}$ with the help of transformation between physical and frequency space. We will use the SOFT package[1] in this work, where the computational cost is $O(N^4)$. Thus, to solve (4.10), we may use conjugate gradient method if $b_k = 0$, and BiCGSTAB or GMRES method for general cases. Furthermore, we may choose constant coefficients A_{kl}, b_k, c, and use the matrix generated by them as a preconditioner for the above methods.

4.2 Parabolic equation

We consider the following parabolic type equation

$$u_t - L_i A_{ij} L_j u + b_i L_i u + f(u) = g(P,t), \tag{4.16}$$

where A_{ij}, b_i are constant, A is symmetric and non-negative, and $|f(x) - f(y)| \leq K|x-y|$. For examples, the propagator equation of a worm-like chain on the sphere, as well as the helical worm-like chain, can be written in this form, with $f(u) = W(P)u$.

As an example, we consider the second-order leapfrog scheme in time:
Let u_N^1 be computed by using a first-order scheme. For $n \leq 1$, we find $u_N^{n+1} \in X_N$ such that

$$\begin{aligned}\frac{1}{2\tau}(u_N^{n+1} - u_N^{n-1}, \phi_N) + A_{ij}\left(L_j\left(\frac{u_N^{n+1}+u_N^{n-1}}{2}\right), L_i\phi_N\right)\\ + \left(b_i L_i\left(\frac{u_N^{n+1}+u_N^{n-1}}{2}\right), \phi_N\right) + (f(u_N^n), \phi_N) = (g(t^n), \phi_N), \quad \forall \phi_N \in X_N.\end{aligned} \tag{4.17}$$

At each time step, one needs to solve an elliptic equation of the kind (4.10) for u_N^{n+1}.

We will use the following discrete Gronwall's inequality (see [15]):

Lemma 4.5. *Suppose $A \geq 0$, and ϕ_n, k_n, g_n are nonnegative sequences satisfying*

$$\phi_n \leq A + \sum_{j=0}^{n-1}(k_j\phi_j + g_j), \quad n \geq 0.$$

Then

$$\phi_n \leq \exp(\sum_{j=0}^{n-1} k_j)(A + \sum_{j=1}^{n} g_j), \quad n \geq 0.$$

Theorem 4.6. *Let u and u_N^{n+1} be the solutions for (4.16) and (4.17), respectively. Then, we have*

$$||u(t^{n+1}) - u_N^{n+1}|| \leq \exp(C_4 T)\Big(\tau^2(||u_{tt}||_{H^1(0,T;L^2)} + ||u_{ttt}||_{L^2(0,T;L^2)}) + N^{-m}||u||_{C(0,T;H^m)}\Big), \tag{4.18}$$

where $C_4 \sim (1 - \tau(1+K^2))^{-1}$.

[1] www.cs.dartmouth.edu/∼geelong/soft/

Proof. We have

$$\frac{1}{2\tau}(\tilde{e}_N^{n+1}-\tilde{e}_N^{n-1},\phi_N)+A_{ij}\left(L_j\left(\frac{\tilde{e}_N^{n+1}+\tilde{e}_N^{n-1}}{2}\right),L_i\phi_N\right) + \left(b_iL_i\left(\frac{\tilde{e}_N^{n+1}+\tilde{e}_N^{n-1}}{2}\right),\phi_N\right)+(f(u(t^n),\phi_N)-f(u_N^n))=(T^n,\phi_N).$$

Let $\phi_N=2\tau(\tilde{e}_N^{n+1}+\tilde{e}_N^{n-1})$, then we have

$$||\tilde{e}_N^{n+1}||^2-||\tilde{e}_N^{n-1}||^2+\frac{\tau}{2}A_{ij}(L_i(\tilde{e}_N^{n+1}+\tilde{e}_N^{n-1}),L_j(\tilde{e}_N^{n+1}+\tilde{e}_N^{n-1})) + 2\tau(f(u(t^n))-f(u_N^n),\tilde{e}_N^{n+1}+\tilde{e}_N^{n-1})=2\tau(T_1^n+T_2^n+T_3^n,\tilde{e}_N^{n+1}+\tilde{e}_N^{n-1}).$$

Now the local truncation errors are given as follows,

$$\begin{aligned}
T_1^n =&\frac{1}{2\tau}(u(t^{n+1})-u(t^{n-1}))-u_t(t^n)=\frac{1}{2\tau}\int_{t^{n-1}}^{t^{n+1}}\frac{1}{2}(s-t^n)^2u_{ttt}\mathrm{d}t,\\
T_2^n =&-L_iA_{ij}L_j\left(\frac{u(t^{n+1})+u(t^{n-1})}{2}-u(t^n)\right)=-L_iA_{ij}L_j\int_{t^{n-1}}^{t^{n+1}}(s-t^n)u_{tt}\mathrm{d}t,\\
T_3^n =&b_iL_i\left(\frac{u(t^{n+1})+u(t^{n-1})}{2}-u(t^n)\right)=\frac{1}{2}b_iL_i\int_{t^{n-1}}^{t^{n+1}}(s-t^n)u_{tt}\mathrm{d}t.
\end{aligned}$$

We have the following estimates,

$$\begin{aligned}
2|(T_1^n,\tilde{e}_N^{n+1}+\tilde{e}_N^{n-1})| &\le ||\tilde{e}_N^{n+1}+\tilde{e}_N^{n-1}||^2+\frac{1}{4\tau^2}||\int_{t^{n-1}}^{t^{n+1}}\frac{1}{2}(s-t^n)^2u_{ttt}\mathrm{d}t||^2\\
&\le ||\tilde{e}_N^{n+1}+\tilde{e}_N^{n-1}||^2+\frac{\tau^3}{40}\int_{t^{n-1}}^{t^{n+1}}||u_{ttt}||^2\mathrm{d}t;\\
2|(T_2^n,\tilde{e}_N^{n+1}+\tilde{e}_N^{n-1})| &= 2|A_{ij}(L_i\int_{t^{n-1}}^{t^{n+1}}(s-t^n)u_{tt}\mathrm{d}t,L_j(\tilde{e}_N^{n+1}+\tilde{e}_N^{n-1}))|\\
&\le \frac{1}{2}A_{ij}(L_i(\tilde{e}_N^{n+1}+\tilde{e}_N^{n-1}),L_j(\tilde{e}_N^{n+1}+\tilde{e}_N^{n-1}))\\
&+2A_{ij}(L_i\int_{t^{n-1}}^{t^{n+1}}(s-t^n)u_{tt}\mathrm{d}t,L_i\int_{t^{n-1}}^{t^{n+1}}(s-t^n)u_{tt}\mathrm{d}t)\\
&\le \frac{1}{2}A_{ij}(L_i(\tilde{e}_N^{n+1}+\tilde{e}_N^{n-1}),L_j(\tilde{e}_N^{n+1}+\tilde{e}_N^{n-1}))+C\tau^3\int_{t^{n-1}}^{t^{n+1}}|u_{tt}|_1^2\mathrm{d}t;\\
2|(T_3^n,\tilde{e}_N^{n+1}+\tilde{e}_N^{n-1})| &\le ||\tilde{e}_N^{n+1}+\tilde{e}_N^{n-1}||^2+C\tau^3\int_{t^{n-1}}^{t^{n+1}}|u_{tt}|_1^2\mathrm{d}t.
\end{aligned}$$

And

$$2|(f(u(t^n))-f(u_N^n),\tilde{e}_N^{n+1}+\tilde{e}_N^{n-1})|\le\ C_1\Big(||\tilde{e}_N^{n+1}||^2+||\tilde{e}_N^{n-1}||^2+||\tilde{e}_N^{n}||^2+||\bar{e}_N^{n}||^2\Big).$$

Thus

$$\begin{aligned}
&||\tilde{e}_N^{n+1}||^2-||\tilde{e}_N^{n-1}||^2\\
&\quad\le C_2\tau(||\tilde{e}_N^{n+1}||^2+||\tilde{e}_N^{n-1}||^2+||\tilde{e}_N^{n}||^2+||\bar{e}_N^{n}||^2)+C_3\tau^4\int_{t^{n-1}}^{t^{n+1}}|u_{tt}|_1^2+||u_{ttt}||^2\mathrm{d}t.
\end{aligned}$$

In the above, $C_2 \lesssim 1 + K^2$. Hence

$$||\tilde{e}_N^{n+1}||^2 \le 3C_2\tau \sum_{k=0}^{n} (||\tilde{e}_N^{k+1}||^2 + ||\bar{e}_N^{k+1}||^2) + C_3\tau^4 \int_0^{t^{n+1}} |u_{tt}|_1^2 + ||u_{ttt}||^2 \mathrm{d}t, \quad n \ge 1.$$

By Gronwall's inequality, if $3C_2\tau < 1$, we have

$$\begin{aligned} ||e_N^{n+1}|| &\le ||\tilde{e}_N^{n+1}|| + ||\bar{e}_N^{n+1}|| \\ &\le \exp(C_4 T)\Big(\tau^2(||u_{tt}||_{H^1(0,T;L^2)} + ||u_{ttt}||_{L^2(0,T;L^2)}) + N^{-m}||u||_{C(0,T;H^m)}\Big). \end{aligned}$$

where $C_4 \sim (1 - 3C_2\tau)^{-1} \sim (1 - \tau(1 + K^2))^{-1}$. □

5 Numerical results

We present in this section several numerical examples to validate our theoretical estimates and to illustrate applications of Wigner D-matrix for solving PDEs on $SO(3)$.

5.1 Elliptic equation

First we examine a stationary equation to test the spatial accuracy. Consider

$$-a_j L_j^2 u + b_j L_j u + cu = f(P). \tag{5.1}$$

The coefficients are chosen as follows:

$$\begin{aligned} &a_1 = 0.5, \quad a_2 = 1, \quad a_3 = 1.5; \\ &b_1 = 0.2, \quad b_2 = 0, \quad b_3 = 0.3; \\ &c = 1. \end{aligned}$$

We choose an exact solution and compute the right-hand term from the equation. Specifically we choose

1. $u_1(P) = (m_{22} - 0.5)^2 |m_{22} - 0.5|$. In this case,

$$\begin{aligned} f_1(P) = 6m_{22}(m_{22} - 0.5)|m_{22} - 0.5| + 3(m_{22} - 0.5)|m_{22} - 0.5|(-0.3m_{12} + 0.2m_{32}) \\ - 6(1.5m_{12}^2 + 0.5m_{32}^2)|m_{22} - 0.5| + (m_{22} - 0.5)^2|m_{22} - 0.5| \in H^1 \backslash H^2. \end{aligned}$$

2. $u_2(P) = \exp(m_{22})$. In this case,

$$f_2(P) = \exp(m_{22})(1 + 0.2m_{32} - 0.3m_{12} + 2m_{22} - 0.5m_{32}^2 - 1.5m_{12}^2) \in C^\infty.$$

The equation is solved using the Galerkin method (4.10). The Wigner coefficients of f is computed using the SOFT package. The error in the L^2-norm is plotted vs. N in Fig. 1 (top). For $f = f_1$, since u_1 and f_1 are not smooth, we observe a convergence rate of N^{-3}, while for $f = f_2$, an exponential convergence is observed since both u_2 and f_2 are smooth. One can check that the convergence rate is consistent with Theorem 4.4.

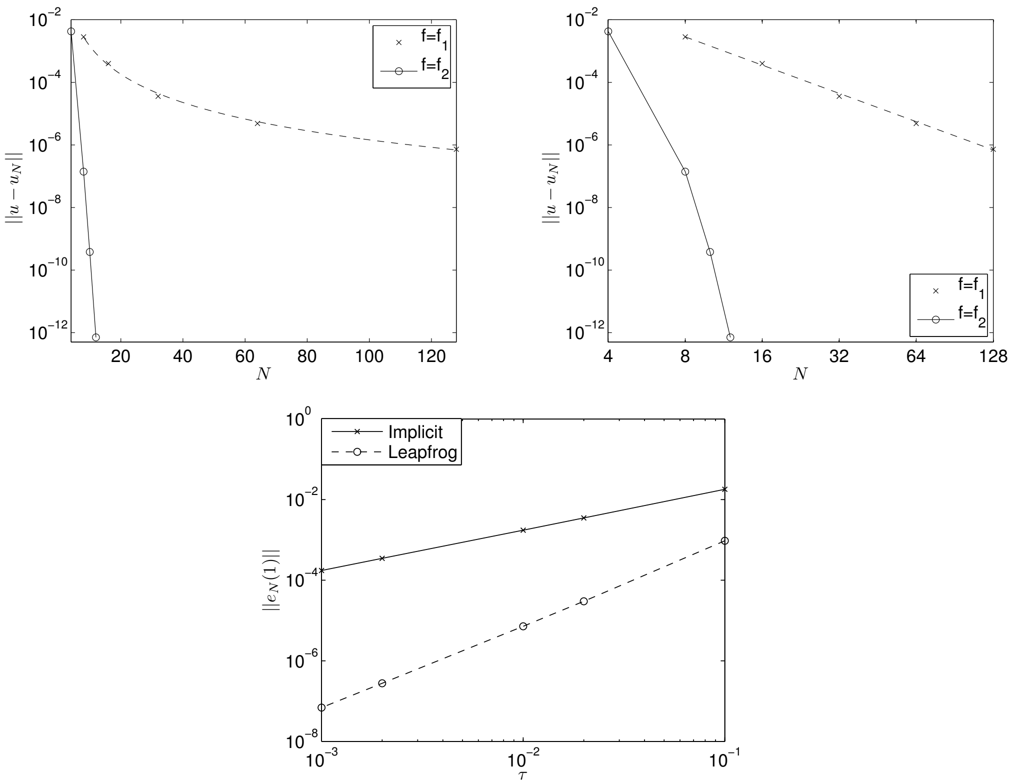

Figure 1: Errors in the L^2-norm. Top: spatial discretization error for the elliptic equation. N is plotted in linear scale (left) and in logarithmic scale (right), respectively. In these two graphs, the dashed lines are a reference curve CN^{-3}. Bottom: Time discretization error for the parabolic equation.

5.2 Parabolic equation

In polymer physics, the equation (4.16) is able to describe the chain propagator, the core of the statistical mechanics of the polymer chain, of helical chains [23] and worm-like chains on spherical surface [13, 14]. In what follows, we examine the equation below,

$$u_t - a_1 L_1^2 u + b_3 L_3 u + W(P)u = 0. \tag{5.2}$$

We first give an example with exact solution to verify the accuracy in time. Then we present another example illustrating how to compute physical quantites from the propagator.

5.2.1 Accuracy test

Here we choose $a_1 = 1$, $b_3 = 0.2$, and let

$$W(P) = -m_{22} + m_{32}^2 + 0.2m_{12} + 1.$$

The initial condition is given by

$$u(P, 0) = \exp(m_{22}).$$

Then the exact solution is

$$u(P, t) = \exp(-t + m_{22}).$$

Since the solution is smooth in space, we choose $N = 16$ so that the spatial error can be ignored and we concentrate on the accuracy in time. The equation is solved till $t = 1$ using and the leapfrog scheme (4.17) and a first-order backward-Euler implicit scheme. To compute $W(P)u(P)$, we use the standard transform (i.e., pseudo-spectral) method [7]. The transforms are also computed using the SOFT package. We compute the error in L^2-norm at $t = 1$, and plot it as a function of τ in Fig. 1 (bottom). It clearly shows that the leapfrog scheme is second-order, compared with the first-order implicit scheme.

5.3 A physical example

We consider a worm-like chain on the spherical surface. We will briefly describe the problem below and refer to [13, 14] for more detailed derivation. We also refer to [5] for a general interpretation of the models for polymer chains.

Suppose that the chain has the length l. The arc length parameter $s \in [0, l]$, referred to as contour length, is used to represent the location of a monomer on the chain. The configuration of the chain is represented by a function $\boldsymbol{r}(s) \in S^2(R)$, describing the location of the monomer s on the sphere of the diameter R. The direction of the monomer s is given by the unit tangent vector $\boldsymbol{u} = \mathrm{d}\boldsymbol{r}/\mathrm{d}s$. The problem can be non-dimensionalized such that we may assume $R = 1$ and $s \in [0, 1]$.

The equation (5.2) of the chain propagator u is derived from the total energy of the worm-like chain, consisting of two parts. In this case, the contour length s is recognized as the time t in (5.2). The first part is the bending energy of the chain, reflected by $-a_1 L_1^2 + b_3 L_3$ in (5.2); the second part is contributed by the monomers in the external field W. Both parts are related to the position $\boldsymbol{r}$ and the direction $\boldsymbol{u}$. For this reason, the propagator is a function of $t = s$ and the pair $(\boldsymbol{r}, \boldsymbol{u})$. Since the chain is on the spherical surface, the tangent vector $\boldsymbol{u}$

must be vertical to $\boldsymbol{r}$. Thus the pair $(\boldsymbol{r},\boldsymbol{u})$ is equivalent to an element in $P\in SO(3)$ if we let $\boldsymbol{r}=\boldsymbol{m}_1(P)$ and $\boldsymbol{u}=\boldsymbol{m}_2(P)$. The parameter $b_3=l/R$ is the ratio of the chain length over the radius of the sphere, and $a_1=1/2\lambda$ is the bending constant of the chain.

The fundamental quantity is the density $\rho(\boldsymbol{r},\boldsymbol{u})=\rho(P)$ of monomers at the position $\boldsymbol{r}$ with the direction $\boldsymbol{u}$. It is calculated from the propagator $u(P)$ and the complementary propagator $u_c(P,t)$, i.e. the propagator starting from the other end of the chain, which satisfies

$$(u_c)_t-a_1L_1^2u_c-b_3L_3u_c+W(PJ)u_c=0,\quad J=\mathrm{diag}(1,-1,-1). \tag{5.3}$$

The initial condition of (5.2) and (5.3) shall be $u(P,0)=u_c(P,0)=1$.

With $u(P)$ and $u_c(P)$, the number density of monomers at contour s is given by

$$\rho(P,s)\propto u(P,s)u_c(P,1-s). \tag{5.4}$$

Hence the number density of monomers, regardless of the contour length, is given by

$$\rho(P)\propto\int_0^1\mathrm{d}s\,\rho(P,s)=\int_0^1\mathrm{d}s\,u(P,s)u_c(P,1-s). \tag{5.5}$$

The normalization constant is given by

$$Z=\int\mathrm{d}P\,u(P,1)=\int\mathrm{d}P\,u(P,s)u_c(P,1-s),\quad\forall s\in[0,1]. \tag{5.6}$$

Thus

$$\rho(P)=\left(\int\mathrm{d}P\,u(P,1)\right)^{-1}\int_0^1\mathrm{d}s\,u(P,s)u_c(P,1-s). \tag{5.7}$$

We choose $a_1=0.3$, $b_3=0.8$, and

$$W(P)=-3\sin^2\beta\cos^2(\gamma-\beta)=-3(m_{31}\sqrt{1-m_{11}^2}-m_{11})^2. \tag{5.8}$$

The discretization parameters are chosen as $\Delta t=0.05$ and $N=16$. At each point on the spherical surface, we compute the number density $\bar{\rho}(\boldsymbol{m}_1)$ of monomers regardless of the direction $\boldsymbol{u}$, and the second-order tensor $Q(\boldsymbol{m}_1)$ describing the orientation,

$$\bar{\rho}(\boldsymbol{m}_1)=\left(2\pi\int\mathrm{d}P\,\rho(P)\right)^{-1}\int\mathrm{d}\gamma\,\rho(P), \tag{5.9}$$

$$Q(\boldsymbol{m}_1)=\left(\int\mathrm{d}\gamma\,\rho(P)\right)^{-1}\int\mathrm{d}\gamma\begin{pmatrix}\cos^2\gamma-\frac12 & \cos\gamma\sin\gamma\\ \cos\gamma\sin\gamma & \sin^2\gamma-\frac12\end{pmatrix}\rho(P). \tag{5.10}$$

The principal eigenvector $\boldsymbol{n}_1$ of Q represents the direction along which the monomers accumulate. The corresponding eigenvalue describes how much they accumulate near $\boldsymbol{n}_1$.

Since W depends only on m_{j1}, we know that $\bar{\rho}(\boldsymbol{m}_1)$ and $\boldsymbol{p}(\boldsymbol{m}_1)$ are functions of m_{11}. Suppose the two polars are chosen as $(\pm1,0,0)$ and the longitudes are connecting the two polars. We plot in Fig. 2 the number density $\bar{\rho}(\boldsymbol{m}_1)$, the principal eigenvalue λ_1, and the angle θ between $\boldsymbol{n}_1$ and the longitudinal line. We can see that under the field (5.8), more monomers appear at low latitudes. Also they accumulate more along $\boldsymbol{n}_1$ at low latitudes. The principal eigenvector $\boldsymbol{n}_1$ is vertical to the longitudinal line at zero latitude, and turns toward the longitudinal line when the longitude grows.

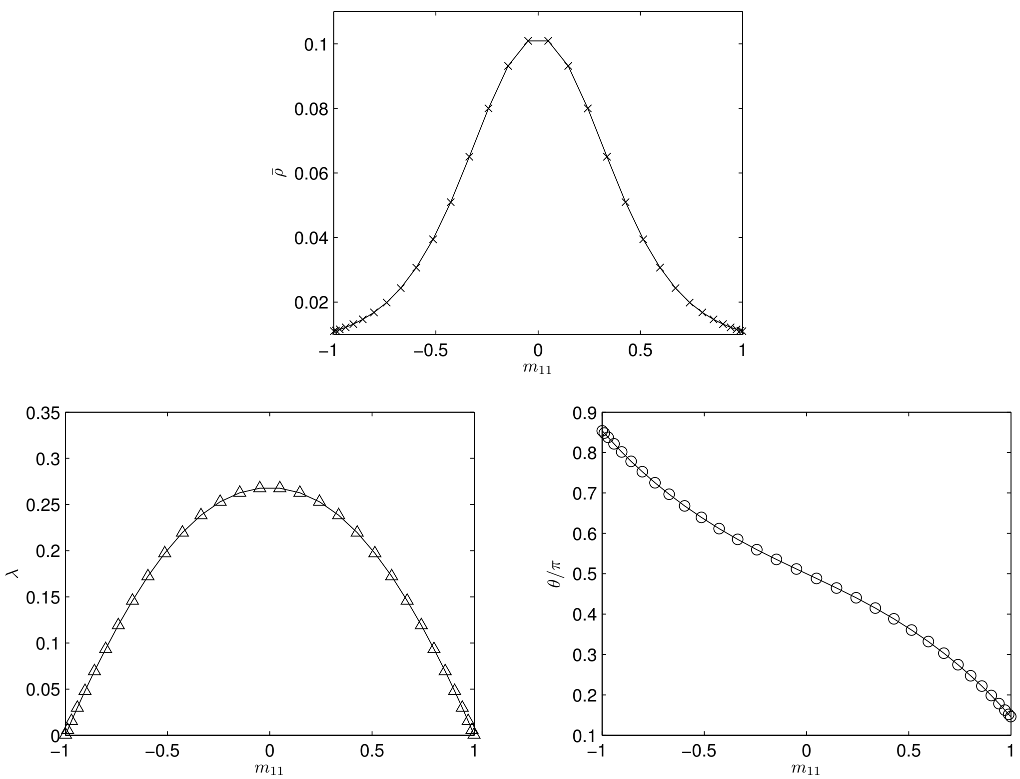

Figure 2: Top: the number density. Bottom left: the principal eigenvalue of Q. Bottom right: the angle between the principal eigenvector and the longitudinal line.

In the self-consistent field theory for polymer, the free energy can be written as a functional of W. Minimizing the free energy gives another equation about W and ρ, forming a closed system together with (5.2) (5.3) and (5.7). When solving the system, the iterating procedure below is followed:

1. Solve the propagators u and u_c from (5.2) and (5.3) for a given field W.

2. Compute from u the density function ρ using (5.7).

3. Update the field W from ρ.

The above procdure is repeated until convergence, which is done in [14]. In every single iteration step, we need to solve (5.2) and (5.3). The accuracy and efficiency is crucial to finding the self-consistent solutions.

6 Concluding remark

Just as spherical harmonic functions are the natural basis for functions on the sphere, Wigner D-matrix forms a natural basis for functions on $SO(3)$. We established in this paper basic approximation results of Wigner D-matrix on $SO(3)$, and showed that they enjoy typical spectral-type of approximation properties. We then developed efficient numerical methods for solving elliptic equations and parabolic equation on $SO(3)$, proved optimal error estimates and present numerical results to validate the numerical algorithms and error estimates. To the best of our knowledge, this is a first paper on the numerical analysis of Wigner D-matrix which plays important role in quantum mechanics and in modeling of liquid crystals and polymers.

The approximation results and basic algorithms presented in this paper will be useful in using Wigner D-matrix for other PDEs on $SO(3)$, particularly those arising from quantum mechanics and in liquid crystal polymers. Indeed, we aim to use the results presented here to approximate Smoluchowski equations of liquid crystals.

Ackowledgment J. Shen is supported in part by NSF DMS-1620262 and AFOSR FA9550-16-1-0102. P. Zhang is supported in part by NSFC grants 11421101 and 11421110001.

References

[1] R. A. Adams. *Soblov Spaces.* Acadmic Press, New York, 1975.

[2] C. Canuto and A. Quarteroni. Approximation results for orthogonal polynomials in Sobolev spaces. *Math. Comp.*, 38:67–86, 1982.

[3] G. S. Chirikjian and A. B. Kyatkin. *Engineering Applications of Noncommutative Harmonic Analysis: With Emphasis on the Rotation and Motion Groups.* CRC Press, Boca Raton, 2001.

[4] M. Doi and S. F. Edwards. *The Theory of Polymer Dynamics.* Oxford University Press, 1986.

[5] G. H. Fredrickson. *The equilibrium theory of inhomogeneous polymers.* Clarendon Press, Oxford, 2006.

[6] T. Funkhouser, P. Min, M. Kazhdan, J. Chen, A. Halderman, D. Dobkin, and D. Jacobs. A search engine for 3D models. *ACM Trans. Graph.*, 22:83–105, 2003.

[7] D. Gottlieb and S. A. Orszag. *Numerical Analysis of Spectral Methods: Theory and Applications.* SIAM-CBMS, Philadelphia, 1977.

[8] B. Guo and L. Wang. Jacobi interpolation approximations and their applications to singular differential equations. *Adv. Comput. Math.*, 14:227–276, 2001.

[9] B. Guo and L. Wang. Jacobi approximations in non-uniformly Jacobi-weighted Sobolev spaces. *J. Approx. Theory*, 128:1–41, 2004.

[10] P. J. Kostelec and D. N. Rockmore. FFTs on the Rotation Group. *J. Fourier Anal. Appl.*, 14:145–179, 2008.

[11] J. A. Kovacs and W. Wriggers. Fast rotational matching. *Acta Crystallographica Section D*, 58:1281–1286, 2002.

[12] H. O. Kreiss and J. Oliger. Stability of the Fourier method. *SIAM J. Numer. Anal.*, 16:421–433, 1979.

[13] Q. Liang, J. Li, P. Zhang, and J. Z. Y. Chen. Modified diffusion equation for the wormlike-chain statistics in curvilinear coordinates. *J. Chem. Phys.*, 138:244910, 2013.

[14] Q. Liang, S. Ye, P. Zhang, and J. Z. Y. Chen. Rigid linear particles confined on a spherical surface: Phase diagram of nematic defect states. *J. Chem. Phys.*, 141:244901, 2014.

[15] A. Quarteroni and A. Valli. *Numerical Approximation of Partial Differential Equations.* Springer-Verlag, Berlin, 2008.

[16] J. Shen, T. Tang, and L. Wang. *Spectral methods*, volume 41 of *Springer Series in Computational Mathematics.* Springer, Heidelberg, 2011. Algorithms, analysis and applications.

[17] S. Sircar, J. Li, and Q. Wang. Biaxial phases of bent-core liquid crystal polymers in shear flows. *Comm. Math. Sci.*, 8:697–720, 2010.

[18] S. Sircar and Q. Wang. Shear-induced mesostructures in biaxial liquid crystals. *Phys. Rev. E*, 78:061702, 2008.

[19] S. Sircar and Q. Wang. Dynamics and rheology of biaxial liquid crystal polymers in shear flow. *J. Rheol.*, 53:819–858, 2009.

[20] N. J. Vilenkin. *Special Functions and the Theory of Group Representations*, volume 22 of *Translations of Mathematical Monographs.* American Mathematical Society, Providence, 1968.

[21] B. D. Wandelt and K. M. Górski. Fast convolution on the sphere. *Phys. Rev. D*, 63:123002, 2001.

[22] E. P. Wigner. *Group Theory and its Application to the Quantum Mechanics of Atomic Spectra*. Academic Press, New York, 1959.

[23] H. Yamakawa and T. Yoshizaki. *Helical Wormlike Chains in Polymer Solutions*. Springer-Verlag, Berlin, 2nd edition, 2016.

[24] D. P. Zelobenko. *Compact Lie groups and their representations*, volume 40 of *Translations of Mathematical Monographs*. American Mathematical Society, Providence, 1973.